APPLIED MECHANICS

A geometrically and physically nonlinear model of a membrane cylindrical shell, which has been built and tested, describes the behavior of a airbag made of fabric material. Based on the geometrically accurate relations of "strain-displacement", it has been shown that the equilibrium equations of the shell, written in terms of Biot stresses, together with boundary conditions acquire a natural physical meaning and are the consequences of the principle of virtual work. The physical properties of the shell were described by Fung's hyper-elastic biological material because its behavior is similar to that of textiles. For comparison, simpler hyper-elastic non-compressible Varga and Neo-Hookean materials, the zero-, first-, and second-order materials were also considered. The shell was loaded with internal pressure and convergence of edges. The approximate solution was constructed by an spectral method; the exponential convergence and high accuracy of the equilibrium equations inherent in this method have been demonstrated. Since the error does not exceed 1 % when keeping ten terms in the approximations of displacement functions, the solution can be considered almost accurate. Similar calculations were performed using a finite element method implemented in ANSYS WB in order to verify the results. Differences in determining the displacements have been shown to not exceed 0.2 %, stresses – 4 %. The study result has established that the use of Fung, Varga, Neo-Hookean materials, as well as a zero-order material, lead to similar values of displacements and stresses, from which displacements of shells from the materials of the first and second orders significantly differ. This finding makes it possible, instead of the Fung material whose setting requires a significant amount of experimental data, to use simpler ones – a zero-order material and the Varga material

Keywords: axisymmetric cylindrical shell, geometric nonlinearity, physical nonlinearity, spectral method

UDC 539.3:517.9
DOI: 10.15587/1729-4061.2021.242372

SPECTRAL SOLUTION TO A PROBLEM ON THE AXISYMMETRIC NONLINEAR DEFORMATION OF A CYLINDRICAL MEMBRANE SHELL DUE TO PRESSURE AND EDGES CONVERGENCE

Vitalii Myntiuk
PhD
Department of Aircraft Strength
National Aerospace University
"Kharkiv Aviation Institute"
Chkalova str., 17, Kharkiv, Ukraine, 61070
E-mail: vitalii.myntiuk@khai.edu

Received date 08.09.2021
Accepted date 08.10.2021
Published date 28.10.2021

How to Cite: *Myntiuk, V. (2021). Spectral solution to a problem on the axisymmetric nonlinear deformation of a cylindrical membrane shell due to pressure and edges convergence. Eastern-European Journal of Enterprise Technologies, 5 (7 (113)), 6–13. doi: https://doi.org/10.15587/1729-4061.2021.242372*

1. Introduction

Shock-absorbing platforms are used to soften the impact when landing cargo or heavy equipment on the Moon, Earth, or another planet. The most widespread platforms, given their simplicity, efficiency, convenience, and cheapness, are those equipped with gas-filled bag. During parachute landing on Earth, cushions are filled with atmospheric air by the energy of the oncoming flow. In order to avoid the rebound of the cargo in the period from the moment the bottom of the bag touches a hard surface until the platform lands, all air must come out of the cushion. During this period, significant pressure is created in the airbag, which causes significant stresses and strains in the material of the airbag. The need to determine them is due to the necessity to calculate the strength, air volume in a deformed airbag, and the area of contact of the airbag with the soil and platform. These parameters are the data required for the design calculations of shock-absorbing systems.

An estimation model of the airbag is a thin membrane shell, which, with rare exception, allows for an accurate solution. Therefore, in practice, it is necessary to apply approximate methods, typically a finite element method (FEM). The disadvantages of this method are the slow convergence of approximate solutions when splitting the grid and, as a result, their low accuracy. These shortcomings are not inherent in the spectral methods that have been advanced due to the use in this work. The implementation of estimation methods alternative to FEM is long overdue.

The task of calculating the shell is greatly complicated by the need to model the physically nonlinear characteristics of the fabric material. The peculiarity of physical laws modeling fabric is a large number of constants that characterize the properties of the material. Determining the constants requires a large number of experiments on specialized equipment, which significantly increases the cost of calculations. Therefore, the numerical-experiment-based substantiation of the possibility to use simpler materials whose involvement does not require a significant experimental base cannot be irrelevant.

2. Literature review and problem statement

Airbag have a variety of shapes, types, and configurations. Paper [1] studied four types of airbag and showed that a cylindrical airbag with a vertical location is most effective in terms of slow-down-magnitude ratio. The dynamic reaction of the airbag of five different shapes was analyzed in work [2]; in study [3], the parameters of the cylindrical airbag were optimized. In the three works cited, simplified thermodynamic modeling of the landing process was ap-

plied, which made it possible to derive analytical solutions. The disadvantage of this approach is that the strain of the airbag is not taken into consideration; this leads to faults in the calculation of volume and makes it impossible to calculate the strength.

To calculate the strain of the airbag, a model with known but rather complex equations of the membrane shell theory is used. These equations are greatly simplified for axisymmetric shells but, for most practically important tasks, they do not allow for accurate solutions. Precise solutions, only when inflating such shells, are based on the use of the first Pipkin integral [4] but, to this end, the shell material must be isotropic.

A significant number of solutions reported in the literature were derived by using FEM. The comparison of finite-element solutions with the experimental data on inflating and longitudinal deformation of the cylindrical shell was carried out in work [5]. A Moony Rivlin material model was used there. In [6], the landing process is simulated using FEM in the LS-DYNA software package in order to further optimize it. The same package is used in works [7, 8] whose authors compare the method of corpuscular particles with the method of volume control and study the effect of mass flow, compression, and the thickness of an airbag on its effectiveness. As already noted, such solutions are universal but inferior in accuracy to the spectral ones.

Among the limited number of works reporting the use of spectral methods, paper [9] is worth noting. In it, the Ritz method was used in counter-variational principles to obtain two-way assessments in the problem of stretching a cylindrical shell made from the Varga and Neo-Hookean materials. Note that displacements of such a shell do not have significant gradients and are rather smooth functions, so the use of a power series up to the fourth order to approximation displacements used in work [9] is permissible. In a more general case, this can lead to significant computational errors.

In most of the cited works, models of rubber-like materials were used while the material of a airbag is a fabric (aviation tarpaulin). This material is characterized by orthotropy since the warp and weft have different mechanical characteristics. That's first. Second, fabrics without coating react to the load in the direction of yarn in two stages. Since the yarn has a wavy shape in a stress-free state, then first there is a strain of the clamp at almost zero load level, and then, as the load level increases, an additional elastic strain appears. These features complicate the modeling of such material. For example, in work [10], the function of additional strain energy is built in the form of a power function of two stresses (along the warp and weft), including nine constants. Paper [11] employed a simpler second-order polynomial, which made it easy to obtain elasticity modules at a predefined level of stress. However, both in the first case and in the second, the resulting functions inadequately represented the test data. The use of the third-order orthotropic model (cubic dependence of strains on stresses) [12] is better at approximating experimental data but requires that 12 constants should be determined.

Work [13] proposed a physical law in which exponential functions are used, it is shown that the strain energy function is available but positive definiteness of the stiffness matrix with significant strains may be lacking. A good correlation of the power model of the material with experimental data was obtained in work [14]. However, strain curves are built for coated fabric material and they are slightly different from curves for uncoated fabrics.

The biological hyper-elastic Fung material was used in [15] because the stretch diagrams of this material and textiles are very similar. There is also a systematic derivation of the relations of the geometrically nonlinear theory of membrane shells using Biot stresses and strains, thereby expanding the series of works by the author on the use of this pair of energetically conjugated tensors in the classical nonlinear theory of shells [16] and beams [17]. In addition, as the review of the literary data shows, spectral methods are hardly used by researchers although their effectiveness has been repeatedly proven. Examples of their successful use can be the solutions to problems of post-buckling behavior of a plate under the action of uniform pressure [18] or convergence of edges [19]. These methods have good prospects and will be applied in the current study.

3. The aim and objectives of the study

The purpose of this work is to build and substantiate an adequate mathematical model of deformation in the cylindrical shell made of textile material and to build an spectral one. This will make it possible to promptly obtain high-precision calculation results with their subsequent use in the design practice.

To accomplish the aim, the following tasks have been set:

– to derive the ratio of "strain-displacement", an equilibrium equation, the boundary conditions, and their corresponding variational principle of virtual work;

– to define the physical law that most accurately simulates the properties of predefined textile material;

– to build an spectral solution;

– to confirm the reliability of the results obtained through a numerical experiment.

4. The study materials and methods

Initially, based on the provisions from the general theory of shells and the nonlinear mechanics of continuum, the relations of "strain-displacement" are built, and the equations of equilibrium Biot stresses are formulated. The same equations are built by direct design of forces and based on the principle of virtual work, which confirms their reliability. Constants in the function of the state of the Fung's hyper-elastic biological material are determined by the method of collocation according to the experimental data given in the literature. An spectral method is used to construct an approximate solution. The accuracy of the solutions is estimated by the magnitude of the non-binding in the equilibrium equations. The reliability of the solutions is confirmed by comparing them with the finite-element solutions obtained by using the ANSYS WB software.

5. Results of studying the physically and geometrically nonlinear axisymmetric deformation of the cylindrical shell

5. 1. Relations of the geometrically nonlinear axisymmetric deformation of the cylindrical shell

The midsurface of the undeformed cylindrical shell is set by the radius-vector r whose components in the rectangular Cartesian coordinate system take the following form (Fig. 1):

$$\mathbf{r}=\left\{r\cos\frac{s}{r},r\sin\frac{s}{r},z\right\}^T, \quad (1)$$

where r is the radius of the shell; s – arc coordinate.

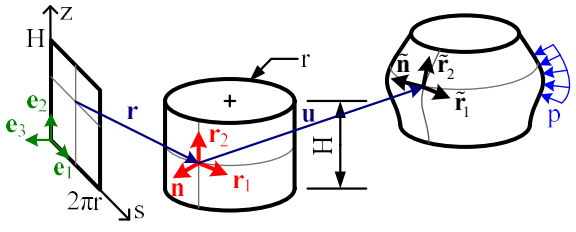

Fig. 1. Dimensions, parameterization, and deformation of the cylindrical shell

The tangent vectors r_α and the normal $\mathbf{n}$ vector (Fig. 1) are determined from the following formulas:

$$\mathbf{r}_1=\partial_1\mathbf{r}=\cos\frac{s}{r}\mathbf{e}_1-\sin\frac{s}{r}\mathbf{e}_3;$$

$$\mathbf{r}_2=\partial_2\mathbf{r}=\mathbf{e}_2;$$

$$\mathbf{r}_3=\mathbf{r}_1\times\mathbf{r}_2=\sin\frac{s}{r}\mathbf{e}_1+\cos\frac{s}{r}\mathbf{e}_3\equiv\mathbf{n}, \quad (2)$$

where the designation $\partial_1(*)\equiv\frac{\partial(*)}{\partial s}$, $\partial_2(*)\equiv\frac{\partial(*)}{\partial z}$. is introduced.

It is not necessary subsequently to distinguish the covariant and contravariant tensor components since r_i form an orthonormalized basis, which, of course, coincides with the mutual one, that is, the first fundamental tensor of the surface is identical to

$$\mathbf{G}=\left\{g_{ij}\right\}=\left\{\mathbf{r}_i\cdot\mathbf{r}_j\right\}=\left\{g^{ij}\right\}=\left\{\mathbf{r}^i\cdot\mathbf{r}^j\right\}=1.$$

All the Christoffel symbols are zero; the Gauss and Weingarten formulas take the following form

$$\partial_1\mathbf{r}_1=-\frac{\mathbf{n}}{r};\quad \partial_1\mathbf{n}=\frac{\mathbf{r}_1}{r}. \quad (3)$$

Thus, the derivative of some arbitrary vector field $\eta=\eta_\beta r_\beta+\eta_3 n$ is calculated by the following formulas

$$\partial_1\eta=\left(\partial_1\eta_1+\frac{\eta_3}{r}\right)r_1+\partial_1\eta_2 r_2+\left(\partial_1\eta_3-\frac{\eta_1}{r}\right)n;$$

$$\partial_2\eta=\partial_2\eta_1 r_1+\partial_2\eta_2 r_2+\partial_2\eta_3 n. \quad (4)$$

In the case of an axisymmetric deformation of the shell, the displacement vector $\mathbf{u}$ would have only two nonzero components

$$\mathbf{u}=v\,\mathbf{r}_2+w\,\mathbf{n}, \quad (5)$$

where v and w are displacements that are set by the functions of one variable – z, the derivative for which is hereafter denoted as $\partial_2 f\equiv\frac{\partial f}{\partial z}\equiv f'$.

The deformation gradient tensor, taking into consideration the rules of differentiation (4), takes the following form

$$\mathbf{F}=1+\frac{\partial\mathbf{u}}{\partial\mathbf{r}}=\left(1+\frac{w}{r}\right)\mathbf{r}_1\mathbf{r}_1+(1+v')\mathbf{r}_2\mathbf{r}_2-$$
$$-k\left(1+\frac{w}{r}\right)(w'\mathbf{r}_2\mathbf{r}_3+(1+v')\mathbf{r}_3\mathbf{r}_3)+w'\mathbf{r}_3\mathbf{r}_2, \quad (6)$$

where k is the norming multiplier of the deformed normal $\tilde{\mathbf{n}}$ (Fig. 1). In the case of the volume invariability hypothesis, k is determined from the condition $\det(\mathbf{F})=1$

$$k=\left[\left(1+\frac{w}{r}\right)^2\left((w')^2+(1+v')^2\right)\right]^{-1}. \quad (7)$$

Polar decomposition of the deformation gradient tensor $\mathbf{F}=\mathbf{Q}\cdot\Lambda$ defines right stretch and proper orthogonal tensor components

$$\Lambda=\sqrt{\mathbf{F}\cdot\mathbf{F}}=\lambda_1\mathbf{r}_1\mathbf{r}_1+\lambda_2\mathbf{r}_2\mathbf{r}_2+\lambda_1^{-1}\lambda_2^{-1}\mathbf{nn}; \quad (8)$$

$$\mathbf{Q}=\mathbf{F}\cdot\Lambda^{-1}=\mathbf{r}_1\mathbf{r}_1+\cos\beta\mathbf{r}_2\mathbf{r}_2-\sin\beta\mathbf{r}_2\mathbf{r}_3+$$
$$+\sin\beta\mathbf{r}_3\mathbf{r}_2+\cos\beta\mathbf{r}_3\mathbf{r}_3, \quad (9)$$

where λ_1, λ_2 are the principal stretches:

$$\lambda_1=1+\frac{w}{r};\quad \lambda_2=\sqrt{(w')^2+(1+v')^2}; \quad (10)$$

$$\cos\beta=\frac{1+v'}{\lambda_2};\quad \sin\beta=\frac{w'}{\lambda_2}; \quad (11)$$

β is the angle of rotation of the deformed normal.

Shell strains, depending on the measure selected, are written as functions of principal stretches. Hereafter, the following is used:

– a logarithmic measure (Genky strains)

$$\varepsilon_\alpha^0=\ln\lambda_\alpha; \quad (12)$$

– the first-order measure (Biot strains)

$$\varepsilon_\alpha=\lambda_\alpha-1; \quad (13)$$

– the second-order measure (Cauchy-Green strains)

$$\varepsilon_\alpha=0.5\left(\lambda_\alpha^2-1\right). \quad (14)$$

The equilibrium equations of the shell element, in the case of using the Biot strain measure (13), take the following form

$$\begin{cases}-(N_2\sin\beta)'+\dfrac{N_1}{r}=p_n;\\ -(N_2\cos\beta)'=p_z,\end{cases} \quad (15)$$

where $N_\alpha=\int_{-h/2}^{h/2}\sigma_\alpha dr$ are the static equivalents of Biot stresses (forces per unit length);

$p_n=p\lambda_1\lambda_2\cos\beta$, $p_z=-p\lambda_1\lambda_2\sin\beta$ – projections of internal pressure p in terms of a deformed midsurface.

Equation (15) can be obtained in different ways. For example, by simplifying known three-dimensional equations [20]

$$\nabla\cdot(\mathbf{Q}\cdot\mathbf{S})^T+\rho\mathbf{f}=0,$$

where $\nabla \cdot \mathbf{A} = \partial_\alpha A_{\alpha\beta}\mathbf{r}_\beta$;

S is the Biot stress tensor;

ρf is the inertial load, which, in a two-dimensional statement of the problem, can simulate pressure.

Equations (15) are derived through the direct mapping of forces (Fig. 2):

– onto the normal n

$$(N_2 + dN_2)dr_1 \sin(\beta + d\beta) - N_2 dr_1 \sin\beta -$$
$$-2N_1 dr_2 \sin\left(\frac{dr_1}{2r}\right) + p_n dr_1 dr_2 = 0;$$

– onto a vertical axis

$$(N_2 + dN_2)dr_1 \cos(\beta + d\beta) - N_2 dr_1 \cos(\beta) +$$
$$+ p_z dr_1 dr_2 = 0.$$

Considering $\sin d\beta = d\beta$, $\cos d\beta = 1$, $\sin\frac{dr_2}{2r} = \frac{dr_2}{2r}$, for small quantities, as well as neglecting the terms of a higher order of smallness, one derives equations (15).

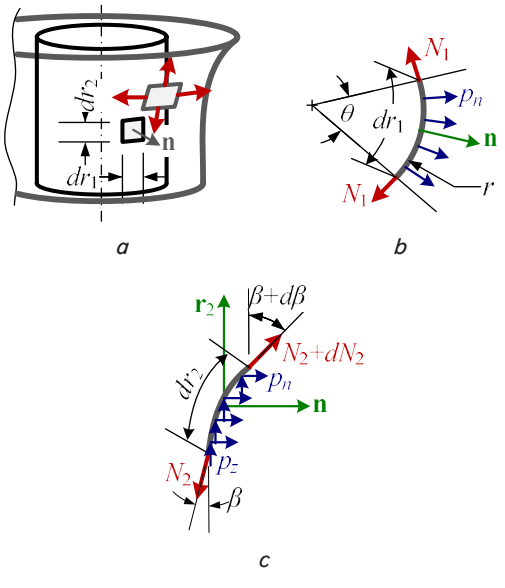

Fig. 2. Equilibrium of the deformed shell element: *a* – position of the shell element; *b* – top view; *c* – side view

In addition, the equilibrium equation can be obtained from the principle of virtual work:

$$0 = \delta A = \int_V \mathbf{S} \cdot \delta\Lambda \, dV - \int_\Sigma \mathbf{p} \cdot \delta u \, d\Sigma =$$
$$= 2\pi r \int_H \left(N_1 \delta\lambda_1 + N_2 \delta\lambda_2 - p_n \delta w - p_z \delta v\right) dz. \qquad (16)$$

If variations of stretches (10) are substituted in (16)

$$\delta\lambda_1 = \frac{\delta w}{r};$$

$$\delta\lambda_2 = \frac{w'}{\lambda_2}\delta w' + \frac{1+v'}{\lambda_2}\delta v' = \delta w' \sin\beta + \delta v' \cos\beta,$$

and, by partial integration, to get rid of derivatives under the sign of variation, one obtains

$$\int_H \left\{ \begin{bmatrix} \frac{N_1}{r} - (N_2 \sin\beta)' - p_n \end{bmatrix} \delta w - \right.$$
$$\left. - \left[(N_2 \cos\beta)' + p_z \right] \delta v \right\} dz +$$
$$+ \left\{ [N_2 \sin\beta] \delta w + [N_2 \cos\beta] \delta v \right\}_{z=0,H} = 0.$$

Due to the independence of variations, this equality holds only when each term in square brackets equals zero. Thus, one derives equilibrium equations (15) and possible boundary conditions at z=0 and z=H:

$$N_2 \sin\beta = 0 \;\vee\; \delta w = 0;$$

$$N_2 \cos\beta = 0 \;\vee\; \delta v = 0. \qquad (17)$$

It should be noted that the principle of virtual work (16) employed an energy-conjugate pair "Biot strains" (13) – "Biot stresses". In the case of other measures of strain (12) or (14) in (16), it is necessary to replace $\delta\lambda_\alpha$ with $\lambda_\alpha^{-1}\delta\lambda_\alpha$ and $\lambda_\alpha \delta\lambda_\alpha$, respectively. At the same time, work will be done by the Kirchhoff stresses (rotated) and the 2nd Piola-Kirchhoff stresses.

Thus, the relations of "displacement-strain" (10), (12) to (14) have been established; a boundary problem has been stated (equilibrium equation (15) and boundary conditions (17)), as well as its corresponding weak formulation (16). To close the system of equations, the relations of "strains-stresses" are required.

5. 2. Physically nonlinear orthotropic material

The state function of the Fung's biological material is set by expression [15]

$$2U = \alpha_1 \varepsilon_1^2 + \alpha_2 \varepsilon_2^2 + 2\alpha_4 \varepsilon_1 \varepsilon_2 + c e^{a_1 \varepsilon_1^2 + a_2 \varepsilon_2^2 + 2a_4 \varepsilon_1 \varepsilon_2}, \qquad (18)$$

where α_1, α_2, α_4, c, a_1, a_2 and a_4 are the constants that determine the properties of the material; $\varepsilon_\alpha = \lambda_\alpha - 1$ – principal strains of the Biot tensor (13).

The constants in (18) were determined by the collocation method, as recommended in [15], according to the experimental data given in [12, 21–23]. The result is the following values: α_1=–180.9 kNm, α_2=–56.3 kNm, α_4=–99.2 kNm, c=12.2 kNm, a_1=15.8, a_2=6.3, a_4=8.1.

Dependence of the forces per unit length

$$N_1 = \frac{\partial U}{\partial \varepsilon_1} = \alpha_1 \varepsilon_1 + \alpha_4 \varepsilon_2 + c\left(a_1 \varepsilon_1 + a_4 \varepsilon_2\right) e^{a_1 \varepsilon_1^2 + a_2 \varepsilon_2^2 + 2a_4 \varepsilon_1 \varepsilon_2},$$

$$N_2 = \frac{\partial U}{\partial \varepsilon_2} = \alpha_2 \varepsilon_2 + \alpha_4 \varepsilon_1 + c\left(a_2 \varepsilon_2 + a_4 \varepsilon_1\right) e^{a_1 \varepsilon_1^2 + a_2 \varepsilon_2^2 + 2a_4 \varepsilon_1 \varepsilon_2} \qquad (19)$$

on strains with different ratios are shown in Fig. 3.

To compare a given material with others, hyper-elastic materials are to be considered:

– Varga [24]

$$U_V = 2\overline{\mu}\left(\lambda_1 + \lambda_2 + \frac{1}{\lambda_2 \lambda_1} - 3\right); \quad N_1 = 2\overline{\mu}\left(1 - \frac{1}{\lambda_2 \lambda_1^2}\right);$$

$$N_2 = 2\overline{\mu}\left(1 - \frac{1}{\lambda_1 \lambda_2^2}\right); \qquad (20)$$

– Neo-Hookean

$$U_{NH}=\bar{\mu}\left(\lambda_1^2+\lambda_2^2+\frac{1}{\lambda_2^2\lambda_1^2}-3\right);\quad \breve{N}_1=\bar{\mu}\left(1-\frac{1}{\lambda_2^2\lambda_1^4}\right);$$

$$\breve{N}_2=\bar{\mu}\left(1-\frac{1}{\lambda_1^2\lambda_2^4}\right); \qquad (21)$$

– the zero-, first-, second-order linear materials

$$U_0=2\bar{\mu}\left(\ln\lambda_1\ln\lambda_2+\ln^2\lambda_1+\ln^2\lambda_2\right);$$

$$\hat{N}_1=2\bar{\mu}\left(2\ln\lambda_1+\ln\lambda_2\right);\quad \hat{N}_2=2\bar{\mu}\left(2\ln\lambda_2+\ln\lambda_1\right); \qquad (22)$$

$$U_1=2\bar{\mu}\left(\lambda_1^2+\lambda_1\lambda_2+\lambda_2^2-3\left(\lambda_1+\lambda_2-1\right)\right);$$

$$N_1=2\bar{\mu}\left(2\lambda_1+\lambda_2-3\right);\quad N_2=2\bar{\mu}\left(2\lambda_2+\lambda_1-3\right); \qquad (23)$$

$$U_2=\frac{\bar{\mu}}{2}\left(\lambda_1^4+\lambda_1^2\lambda_2^2+\lambda_2^4-3\left(\lambda_1^2+\lambda_2^2-1\right)\right);$$

$$\breve{N}_1=\bar{\mu}\left(2\lambda_1^2+\lambda_2^2-3\right);\quad \breve{N}_2=\bar{\mu}\left(2\lambda_2^2+\lambda_1^2-3\right); \qquad (24)$$

where $\bar{\mu}=\mu h$ is the shear module per unit length; $\breve{N}_\alpha=N_\alpha\lambda_\alpha$, $\hat{N}_\alpha=N_\alpha\lambda_\alpha^{-1}$ – static equivalents of the 2nd Piola-Kirchhoff stresses and the rotated Kirchhoff stresses.

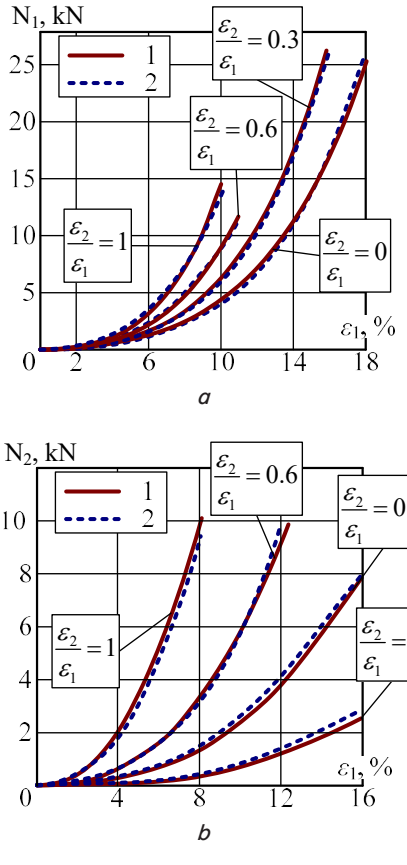

Fig. 3. Modeling of experimental data: *a* – dependence of the force N_1 per unit length on strain; *b* – dependence of the force N_2 per unit length on strain; 1 – state function (18); 2 – experimental data [22]

5. 3. Spectral solution

The desired displacement functions $v(z)$ i $v(z)$ ($z=-H/2...H/2$) in the case of setting nonhomogeneous essential boundary conditions (17) are built in the form of sums

$$v(z)=V_{01}\left(\frac{1}{2}-\frac{z}{H}\right)+V_{02}\left(\frac{1}{2}+\frac{z}{H}\right)+\sum_{i=0}V_i\varphi_i(z);$$

$$w(z)=W_{01}\left(\frac{1}{2}-\frac{z}{H}\right)+W_{02}\left(\frac{1}{2}+\frac{z}{H}\right)+\sum_{i=0}W_i\psi_i(z). \qquad (25)$$

where V_{01}, V_{02}, W_{01}, W_{02} are the displacement magnitudes specified at the boundary;

V_i, V_i – the coefficients to be determined using variational methods;

$\varphi_i(z)$, $\psi_i(z)$ – known basic functions.

The basis functions taken are those functions whose derivatives are orthogonal in the metric L_2 [25, 26]

$$\varphi_i(z)=\psi_i(z)=P_{i+2}\left(\frac{2z}{H}\right)-P_i\left(\frac{2z}{H}\right). \qquad (26)$$

Here, P_i is the Legendre polynomials.

Coefficients in sums (25) are determined by solving a system of nonlinear algebraic equations, which is followed from the principle of virtual work (16). The system of equations is solved by the Newton method.

5. 4. Numerical experiment

As a test problem, the cylindrical shell under internal pressure is considered, with its edges converging. The shell dimensions are H=0.77 m, r=0.53 m. The conditional thickness, calculated as the ratio of density to mass per square meter, is equal to h=0.804 mm. The value of the internal pressure is p=100 kPa, the convergence of edges is Δ=0.35 m. In the case of using materials (20) to (24), the shear module μ=92.248 MPa ($\bar{\mu}$=74.208 kN/m), which corresponds to the effort of 1.78 kN when stretching a strip 5 cm wide by 16 %.

Since an approximate solution is being built, first of all, it is necessary to assess the convergence and accuracy of the results. Fig. 4, *a* shows the convergence of the maximum deflection of the shell w, and the maximum force N_1 value, depending on the number of unknown K coefficients in sums (25). For reference values, the corresponding values at the top index in the sums equal to 12 were taken. Since the solutions are quite smooth, the expected exponential convergence is observed. Fig. 4, *b* shows the inconsistencies in equilibrium equations (15). As one can see, their highest value does not exceed 1 % when keeping 10 terms in sums (25) (K=20), that is, the approximate solution can be considered almost precise.

The reliability of the results is confirmed by comparing the deflections and efforts obtained by the proposed method and FEM implemented in the ANSYS WB software [27]. The relative difference in determining the displacement does not exceed 0.2 %, stresses – 4 %.

Deformed meridians of the cylindrical shell when using various materials are shown in Fig. 5. As one can see, the use of linear materials of the first and second orders leads to a decrease in deflections and an increase in longitudinal displacements. Note that these materials are not non-compressible although the Poisson coefficient is set to 0.5. For the rest of the materials, the non-compressibility hypothesis is fair, the deformation of the shells made of these materials is similar.

A similar pattern is observed for the distribution of forces per unit length (Fig. 6). For comparison, all forces were reduced to the static equivalents of engineering stresses, that is, the Piola-Kirchhoff stresses were recalculated according to the formula $\lambda_\alpha^{-1}\breve{N}_\alpha$, the rotated Kirchhoff stresses – $\lambda_\alpha\hat{N}_\alpha$.

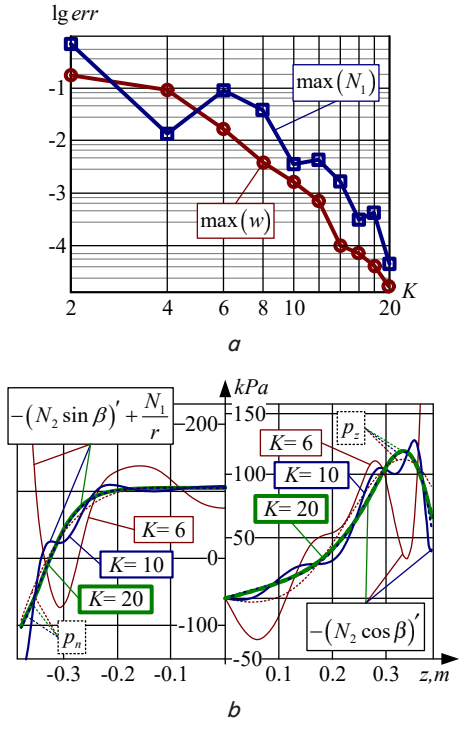

Fig. 4. Convergence and accuracy of the approximate solution: *a* – dependence of the error in determining the maximum deflection and stresses; *b* – values of the left- and right-hand sides of equilibrium equations (15) while keeping 6, 10, and 20 unknowns in sums (25)

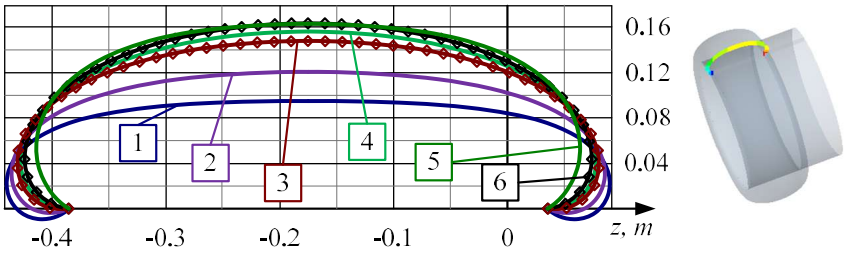

Fig. 5. Deformed meridians of the cylindrical shell: 1 – linear material of the second order (24); 2 – linear material of the first order (23); 3 – Neo-Hookean material (21), ANSYS WB; 4 – Varga material (20); 5 – Fung material (18); 6 – zero-order linear material (22), ANSYS WB

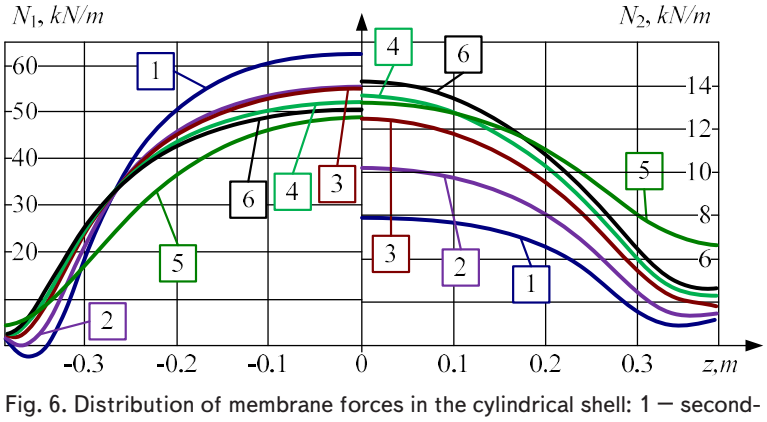

Fig. 6. Distribution of membrane forces in the cylindrical shell: 1 – second-order linear material (24); 2 – linear material of the first order (23); 3 – Neo-Hookean material (21), ANSYS WB; 4 – Varga material (20); 5 – Fung material (18); 6 – zero-order linear material (22), ANSYS WB

As one can see, the second-order linear material produces significantly inflated values of tangential stresses and understated longitudinal ones. The tangential stresses in the shell made of the first-order linear material almost coincide with the stresses in the Neo-Hookean shell, but the longitudinal stresses are underestimated.

The compliance of Fung material at small strains is most pronounced in areas near the edges of the shell (Fig. 5). In these zones, the shell is less loaded (Fig. 6), so the difference in the values of displacements and stresses is more significant. If the task of determining the maximum strains and stresses is set, then replacing Fung's material with a zero-order material leads to an error in determining the maximum deflection of 0.2 %, and the maximum stress – 3 %.

6. Discussion of results of studying the shell strain deformation

The simplicity and clarity of geometrically nonlinear relations (15) to (17) are due to the use of an energy-conjugated pair of tensors of the Biot strains and stresses (13), which have a clear engineering interpretation: engineering stresses and stretch ratio. The high accuracy of the approximate solution (Fig. 4) is explained by the use of an spectral method with a polynomial approximation of displacement functions (25). To obtain an almost accurate solution, it took the introduction of 20 unknowns, this is almost an order of magnitude less compared to FEM (with an element size of 10 mm and quadratic interpolation).

The similarity in the shapes of the deformed shell made from different materials (Fig. 5) can be explained by similar physical properties of these materials in the predefined zone of "stresses-strains". Almost all shell material is in the most stressed zone, except for the zones at the edges of the shell (Fig. 6) where the differences in deformations are greater (Fig. 5).

Features of textile behavior are well modeled by the Fung biological hyper-elastic material (18), (19). The disadvantage of using this material is the need for a significant amount of experimental data. It is possible to replace this material with simpler ones: the zero-order single-constant materials (22) and Varga (20), which does not lead to significant errors in determining displacements and stresses. Applying the second-order material (24) significantly overestimates the rigidity of the shell, resulting in significant errors both in determining the displacements and determining the stresses. Its use in problems of this type is undesirable.

With significant compression of the shell or reduced pressure, negative stress values appear, which is unacceptable for fabrics. This limits the use of a given model. The formation of folds is modeled either by shells with nonzero bending rigidity, which significantly complicates the model or in a simplified way – by introducing the energy function of a relaxed strain [28].

The disadvantage of the current study is disregarding the nonlinearity of the third type – contact. When landing, the airbag inevitably comes into contact with the

soil, platform, or adjacent airbag. Failure to account for these phenomena can significantly affect the results.

The removal of the noted restrictions and the elimination of shortcomings indicate the directions of further development of this study.

7. Conclusions

1. The geometrically nonlinear relations have been constructed in terms of the Biot strains and stresses, that is, regular stretch ratios and engineering stresses. The advantage of their use is, first, the convenience of processing experimental data and, second, a clear interpretation of the equilibrium equations, shown in this work. The main disadvantage of using this pair (the need to extract the root from the square of the deformation gradient tensor) is not significant, in this case. The exact expressions of the stretch and rotation tensors components take a compact form, do not require any simplifications, and their subsequent use leads to the geometrically accurate equilibrium equations, boundary conditions, and variational principles.

2. Fung's material takes into consideration orthotropy and correlates well with the data from experiments on two-axial stretching of fabric materials. The discrepancy between the experimental and approximated stress values is less than 8 %.

3. The orthogonality of the function's derivatives, which were used in the construction of spectral solutions, in the L_2 metric leads to well-conditioned matrices in the energy metric of the differential operator of a given boundary problem. The inconsistency in the equilibrium equations does not exceed 1 % when keeping ten terms in the approximation of displacement functions, that is, the resulting solutions can be considered almost accurate.

4. The reliability has been confirmed by comparing the results obtained with the results obtained when using FEM. Differences in determining the displacements do not exceed 0.2 %, stresses – 4 %.

Acknowledgments

This study is supported by the Ministry of Education and Science of Ukraine within the framework of research project No. 0121U109604.

References

1. Esgar, J. B., Morgan, W. C. (1960). Analytical Study of Soft Landings on Gas-filled Bags. NASA TR R-75. U.S. Government Printing Office, 30. Available at: https://books.google.com.ua/books/about/Analytical_Study_of_Soft_Landings_on_Gas.html?id=k28A2nzFGVoC&redir_esc=y
2. Alizadeh, M., Sedaghat, A., Kargar, E. (2014). Shape and Orifice Optimization of Airbag Systems for UAV Parachute Landing. International Journal of Aeronautical and Space Sciences, 15 (3), 335–343. doi: https://doi.org/10.5139/ijass.2014.15.3.335
3. Zhou, X., Zhou, S. M., Li, D. K. (2019). Optimal Design of Airbag Landing System without Rebound. IOP Conference Series: Materials Science and Engineering, 531, 012001. doi: https://doi.org/10.1088/1757-899x/531/1/012001
4. Pipkin, A. C. (1968). Integration of an equation in membrane theory. Zeitschrift Für Angewandte Mathematik Und Physik ZAMP, 19 (5), 818–819. doi: https://doi.org/10.1007/bf01591012
5. Pamplona, D. C., Gonçalves, P. B., Lopes, S. R. X. (2006). Finite deformations of cylindrical membrane under internal pressure. International Journal of Mechanical Sciences, 48 (6), 683–696. doi: https://doi.org/10.1016/j.ijmecsci.2005.12.007
6. Wang, H., Hong, H., Hao, G., Deng, H., Rui, Q., Li, J. (2014). Characteristic verification and parameter optimization of airbags cushion system for airborne vehicle. Chinese Journal of Mechanical Engineering, 27 (1), 50–57. doi: https://doi.org/10.3901/cjme.2014.01.050
7. Zhou, M., Di, C., Yang, Y. (2017). Simulation of Cushion Characteristic of Airbags Based on Corpuscular Particle Method. Proceedings of the 2017 2nd International Conference on Automation, Mechanical Control and Computational Engineering (AMCCE 2017). doi: https://doi.org/10.2991/amcce-17.2017.34
8. Li, Y., Xiao, S., Yang, B., Zhu, T., Yang, G., Xiao, S. (2018). Study on the influence factors of impact ejection performance for flexible airbag. Advances in Mechanical Engineering, 10 (10), 168781401880733. doi: https://doi.org/10.1177/1687814018807333
9. Haddow, J. B., Favre, L. Ogden, R. W. (2000). Application of variational principles to the axial extension of a circular cylindical nonlinearly elastic membrane. Journal of Engineering Mathematics 37, 65–84. doi: https://doi.org/10.1023/A:1004709622104
10. Chen, Y., Lloyd, D. W., Harlock, S. C. (1995). Mechanical Characteristics of Coated Fabrics. Journal of the Textile Institute, 86 (4), 690–700. doi: https://doi.org/10.1080/00405009508659045
11. Yang, B., Yu, Z., Zhang, Q., Shang, Y., Yan, Y. (2020). The nonlinear orthotropic material model describing biaxial tensile behavior of PVC coated fabrics. Composite Structures, 236, 111850. doi: https://doi.org/10.1016/j.compstruct.2019.111850
12. Farboodmanesh, S., Chen, J., Tao, Z., Mead, J., Zhang, H. (2019). Base fabrics and their interaction in coated fabrics. Smart Textile Coatings and Laminates, 47–95. doi: https://doi.org/10.1016/b978-0-08-102428-7.00003-1
13. Hegyi, D., Halász, M., Molnár, K., Szebenyi, G., Sipos, A. A. (2017). An elastic phenomenological material law for textile composites and it's fitting to experimental data. Journal of Reinforced Plastics and Composites, 36 (18), 1343–1354. doi: https://doi.org/10.1177/0731684417707586
14. Wang, C., Cao, X., Shen, H. (2021). Experimental and Numerical Investigation of PA66 Fabrics Coated/Uncoated PVC by Biaxial Tensile Tests. Fibers and Polymers, 22 (8), 2194–2205. doi: https://doi.org/10.1007/s12221-021-0122-y
15. Fung, Y.-C. (1993). Biomechanics. Mechanical Properties of Living Tissues. Springer, 568. doi: https://doi.org/10.1007/978-1-4757-2257-4

16. Myntiuk, V. B. (2018). Biot Stress and Strain in Thin-Plate Theory for Large Deformations. Journal of Applied and Industrial Mathematics, 12 (3), 501–509. doi: https://doi.org/10.1134/s1990478918030109
17. Khalilov, S. A., Myntiuk, V. B. (2018). Postbuckling Analysis of Flexible Elastic Frames. Journal of Applied and Industrial Mathematics, 12 (1), 28–39. doi: https://doi.org/10.1134/s1990478918010040
18. Myntiuk, V. B. (2020). Postbuckling of a Uniformly Compressed Simply Supported Plate with Free In-Plane Translating Edges. Journal of Applied and Industrial Mathematics, 14 (1), 176–185. doi: https://doi.org/10.1134/s1990478920010160
19. Kravchenko, S. G., Myntiuk, V. (2020). Nonlinear Postbuckling Behavior of a Simply Supported, Uniformly Compressed Rectangular Plate. Advances in Intelligent Systems and Computing, 35–44. doi: https://doi.org/10.1007/978-3-030-37618-5_4
20. Reddy, J. N. (2013). An Introduction to Continuum Mechanics. Cambridge: Cambridge University Press, 450. doi: https://doi.org/10.1017/cbo9781139178952
21. Day, A. S. (1986). Stress strain equations for non-linear behaviour of coated woven fabrics. IASS Symposium Proceedings: Shells, Membranes and Space Frames, 17–24.
22. Kawabata, S., Niwa, M., Kawai, H. (1973). 3–The Finite-Deformation Theory of Plain-Weave Fabrics Part I: the Biaxial-Deformation Theory. The Journal of The Textile Institute, 64 (1), 21–46. doi: https://doi.org/10.1080/00405007308630416
23. Buet-Gautier, K., Boisse, P. (2001). Experimental analysis and modeling of biaxial mechanical behavior of woven composite reinforcements. Experimental Mechanics, 41 (3), 260–269. doi: https://doi.org/10.1007/bf02323143
24. Varga, O. H. (1966). Stress-strain Behavior of Elastic Materials. Interscience Publishers, 190.
25. Shen, J. (1994). Efficient Spectral-Galerkin Method I. Direct Solvers of Second- and Fourth-Order Equations Using Legendre Polynomials. SIAM Journal on Scientific Computing, 15 (6), 1489–1505. doi: https://doi.org/10.1137/0915089
26. Mintyuk, V. (2007). Ortonormirovanniy bazis dlya odnomernyh kraevyh zadach. Aviacionno-kosmicheskaya tehnika i tehnologiya, 5 (41), 32–36. Available at: http://nti.khai.edu:57772/csp/nauchportal/Arhiv/AKTT/2007/AKTT507/Mintjuk.pdf
27. Ansys®. Academic Research Mechanical, Release 21.2. Available at: https://www.ansys.com/
28. Tait, R., Connor, P. (1997). On the expansion of a deformed cylindrical elastic membrane. IMA Journal of Applied Mathematics, 59 (3), 231–243. doi: https://doi.org/10.1093/imamat/59.3.231